



A grain boundary model of metamorphic reaction

Frank S. Spear¹

Received: 21 October 2023 / Accepted: 14 January 2024 / Published online: 15 March 2024
© The Author(s) 2024

Abstract

A model is presented whereby metamorphic parageneses are governed by local, nano-scale reactions among adjacent phases along grain boundaries that are driven by local disequilibrium between the solid phases and the grain boundary composition. These reactions modify the grain boundary composition setting up compositional gradients that drive diffusion and change the grain boundary composition elsewhere in the rock, which drive local reactions in these locations. The process may be triggered by the nucleation of a new phase that is out of equilibrium with the existing assemblage and an example is presented based on the transformation of kyanite (Ky) to sillimanite (Sil). Model results reveal that a simple polymorphic transformation (Ky→Sil) can result in local reactions among all phases in the rock and some phases may grow in one locale and be consumed in another. An implication of these results is that interpretation of metamorphic parageneses based on growth or resorption and compositional changes of phases requires careful evaluation of nano-scale processes.

Keywords Kyanite = Sillimanite · Grain boundary diffusion · Metamorphic reaction modeling

Introduction

Metamorphic reactions can only proceed if there is a driving force. Whereas it is often assumed that progressive metamorphism proceeds as a series of near-equilibrium steps, there is a growing body of evidence that considerable overstepping is required for the nucleation of a new phase. Inferences about degrees of overstepping are not new and have been promoted as explanation of certain paragenetic relations for decades. Hollister (1969a, b), for example, concluded that considerable overstepping of the Al_2SiO_5 phase boundaries was required to explain the observed occurrences of kyanite, andalusite, and sillimanite. More recent studies have suggested that phases such as garnet, staurolite, kyanite, and sillimanite all require considerable overstepping before nucleating (Pattison et al. 2011; Pattison and Spear 2018; Spear et al. 2014; Spear and Wolfe 2022; Castro and Spear 2017; Wolfe and Spear 2018; Waters and Lovegrove 2002; Chu et al. 2023). Indeed, Pattison and Spear (2018),

Spear and Pattison (2017) and Pattison (2023) has argued that it is difficult to explain typical Barrovian metamorphic sequences in the absence of considerable overstepping before the nucleation of these phases.

The amount of overstepping required for the nucleation of any specific phase is under debate. Rather than formulate overstepping in terms of ΔT or ΔP relative to the equilibrium phase boundary, it is a convenient means of normalization to define overstepping in terms of affinity. Affinity in this context is defined as the difference between the free energy of a phase yet to nucleate and the free energy as defined by the phase-free assemblage. Graphically, this corresponds to the free energy difference between the tangent to the existing phase-free assemblage and the parallel tangent to the fictive phase—the so-called “parallel tangent” approach (e.g., Thompson and Spaepen 1983; Pattison et al. 2011; Gaidies et al. 2011; Spear et al. 2014). Reported as Joules/mol-O, this approach provides a means of comparing the degree of overstepping of different phases with different numbers of oxygens in their formulas.

Pattison et al. (2011) have suggested a value of a few hundred J/mol-O as a threshold for nucleation of garnet. Spear and Wolfe (2022) have reported values ranging from a few hundred to several thousand J/mol-O for the nucleation of garnet in metapelites and quartzites from New England (see also Table 7 in Chu et al. 2023 for a summary

Communicated by Dante Canil.

✉ Frank S. Spear
spearf@rpi.edu

¹ Department of Earth and Environmental Sciences,
Rensselaer Polytechnic Institute, 110 8th Street, Troy,
NY 12180, USA

of reported values). The requirements for a new phase to nucleate are therefore not at all well-determined. However, it is clear from these studies that after a phase such as garnet, staurolite, kyanite or sillimanite has nucleated, it is out of equilibrium with the preexisting assemblage and the system must react in an attempt to re-establish equilibrium.

The purpose of this paper is to present a model for the evolution of metamorphic recrystallization when a new phase nucleates and is out of equilibrium with the preexisting assemblage. The example used to illustrate this model is the simple kyanite = sillimanite reaction that occurs in a typical prograde Barrovian sequence in metapelites. A key facet of the model is the assumption that reaction kinetics are relatively fast, but reactions are local in extent and only occur among adjacent phases. The overall mineralogical evolution of the assemblage is therefore controlled largely by grain boundary diffusion.

The physical model

There is a large literature on the kinetics of reactions as applied to metamorphic systems (for a superb summary of this literature and models, see Gaidies et al., 2017). The two end-member kinetic models are interface-controlled reactions and diffusion-controlled reactions. For interface-controlled reactions, it is assumed that either the attachment of atoms to a growing crystal or the detachment of atoms from a crystal being consumed is the rate-limiting step and that the diffusion of elements to or from the growing crystal is rapid. For diffusion-controlled reaction kinetics, it is assumed that the interface reactions are essentially instantaneous and the growth or consumption of crystals is dictated by the rate of diffusion to or from the reaction sites.

The model described here is based on the assumption that metamorphic reactions occur only on a very local (nanometer) scale and that communication between local reaction sites occurs through grain boundary diffusion. That is, the model assumes the interface kinetics are rapid although highly localized and the rate-limiting step is grain boundary diffusion. It should be emphasized that it is not intended to argue that interface kinetics are rapid in all types of metamorphic reactions. Rather, the intention is to explore the consequences of grain boundary diffusion as the rate-limiting step on the evolution of metamorphic textures. Figure 1 shows a cartoon of the imagined grain boundary configuration in two dimensions in a rock containing muscovite, quartz, and sillimanite or kyanite. Reactions are assumed to occur only between adjacent phases (muscovite + quartz, muscovite + Al_2SiO_5 , or quartz + Al_2SiO_5) or among three phases at 3-grain intersections (muscovite + quartz + Al_2SiO_5). These local reactions are essentially open-system reactions (open to the grain boundary

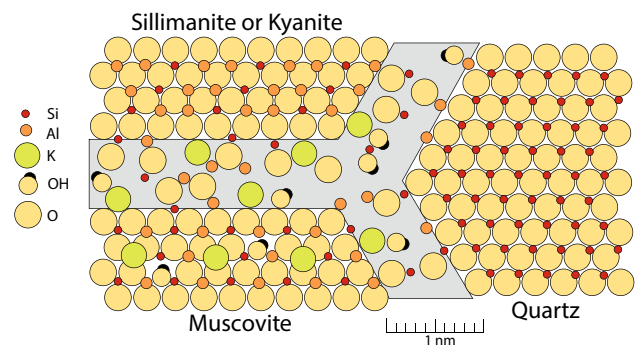


Fig. 1 Schematic drawing of a hypothetical grain boundary at the junction of muscovite, quartz, and kyanite or sillimanite in the system KASH. The grain boundary is assumed to be approximately 1 nm wide and contain unspecified concentrations of the system cations. Oxygens in the grain boundaries are loosely bonded to the nearby crystal lattice. Note that the lattice arrangement in the solid phases is schematic

elements) and require balancing on one or more elements, which is accomplished in this model by balancing on oxygen. Grain boundaries are constrained to not grow or shrink in width, which is also accomplished by conserving oxygen among reacting solid phases. It is important to note that balancing reactions based on the conservation of oxygen does not in any way imply that oxygen is immobile only that the amount of oxygen in the grain boundary phase is constant and the growth of one oxide (e.g., sillimanite) is limited by the oxygen supplied by the adjacent oxide (e.g., quartz or muscovite). A detailed discussion of the thermodynamic calculations on which the reaction modeling is based is presented below.

The result of local reaction is the growth or consumption of adjacent phases and modification of the grain boundary composition with this new grain boundary composition determined by the local reaction stoichiometry. Local modification of the grain boundary composition sets up compositional gradients along the grain boundary which drives diffusion, and this diffusion results in modification of the grain boundary composition elsewhere in the rock, which serves to drive local reactions at these new locations. A discussion of the methodology to implement the grain boundary diffusion is presented below.

The model is constructed as a two-dimensional grid with phases occupying polygons separated by grain boundaries and connected by nodes (Fig. 2). Following each episode of reaction, phases may either grow or be consumed and the grid is modified to accommodate the change in modal amounts. A detailed description of the construction and modification of the grid is given in the Appendix I.

The model presented here differs from previous models that invoke grain boundary diffusion as the rate-limiting step in several ways (e.g., Carlson 1989, 1991, 2002; Foster 1986,

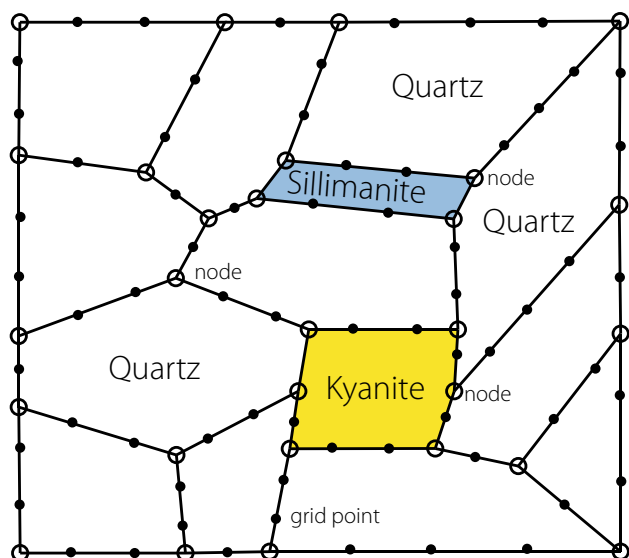


Fig. 2 Simplified example of a model grid in the system $\text{SiO}_2 - \text{Al}_2\text{O}_3$ containing only the phases quartz, sillimanite, and kyanite. Grain boundaries are divided up into segments with individual grid points (black dots) and nodes are where 2 or 3 grain boundaries join (open circles)

1990; Gaidies et al. 2011, 2017). First, it is assumed here that diffusion occurs only along grain boundaries. This is not to imply that intracrystalline diffusion either within a phase or between phases and adjacent grain boundaries does not occur, but rather that diffusive exchange between phases and the adjacent grain boundary is negligible. Second, restricting diffusion to occur only along grain boundaries is fundamentally different from previous models of diffusion control in which diffusion is through a medium such as a rock “matrix” or a melt or aqueous solution (e.g., Carlson 1989, 1991; Gaidies et al., 2017). Third, it is assumed that the transport of material along grain boundaries does not involve an aqueous phase so relative solubilities of species in an aqueous phase is not considered (e.g., Carlson et al. 2015). Rather, transport along grain boundaries is modeled strictly as a one-dimensional diffusive flux. Finally, this is the first model of its type that specifically incorporates the spatial arrangement of reacting phases with the objective of monitoring the evolution of the mineralogical texture.

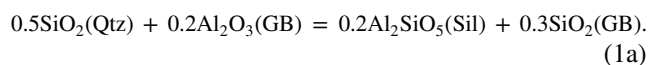
Reaction modeling

Phase reactions are considered to occur only where two or three phases are adjacent along a grain boundary or a node. Grain boundaries are constrained to not grow in width during reaction. This is achieved in the model by balancing each local reaction on oxygen. Similar results would be obtained by balancing reactions to specifically conserve volume, but

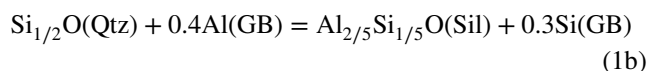
balancing on oxygen is mathematically simpler. As shown in Fig. 1, grain boundaries are assumed to contain both cations and oxygen and the distribution of species on grain boundaries is undoubtedly very complex. However, balancing on oxygen simply ensures that the overall amount of oxygen in the grain boundary is constant and that the width of the grain boundary will not change significantly as reactions proceed. The driving force for reaction progress is the thermodynamic affinity between the reacting solid phases and the grain boundary “phase”. Reactions are permitted to proceed until the affinity among the reacting phases is identical, at which point there will no longer be a driving force for the production or consumption of a solid phase.

The theoretical background for this approach to monitoring reaction progress is depicted graphically in Fig. 3. Consider the system Al–Si–O containing the phases quartz, kyanite, sillimanite, and the grain boundary (GB). The phases plot on the Al–Si–O triangle as shown in Fig. 3a. Although the amount of oxygen in the grain boundary (GB) is not known and most probably varies from location to location, the grain boundary is shown in Fig. 3a as containing less oxygen than the solid phases, which are largely close-packed arrays of oxygen, and many of the cations in the grain boundary will be loosely bonded to under-bonded oxygens in adjacent phases (Fig. 1).

The G–X diagram (Fig. 3b) shows the tangent line kyanite–quartz–GB in blue. Assume that the P–T conditions are in the sillimanite field so that sillimanite has a lower free energy than kyanite but has not yet nucleated. Assuming that the rock is initially in equilibrium, kyanite, quartz, and the grain boundary “phase” all plot on the common tangent shown in blue in Fig. 3b. Now assume that sillimanite nucleates and shares a grain boundary with quartz. Sillimanite is out of equilibrium with the local grain boundary composition and quartz and sillimanite will react by the oxygen-conserving reaction:



Since the amount of oxygen in the grain boundary is constant, this reaction can be more readily understood by simplifying the representation of the grain boundary components to include only cations and recast the formulas for the solid phases to include only 1 oxygen:



The grain boundary composition becomes depleted in Al and enriched in Si as sillimanite is produced. The eventual G–X configuration when the reaction runs to completion is shown in Fig. 3b in red. Note that the tangent to the grain boundary (dashed red line) is not, in general, coincident with the quartz–sillimanite tangent (solid red line) but rather the

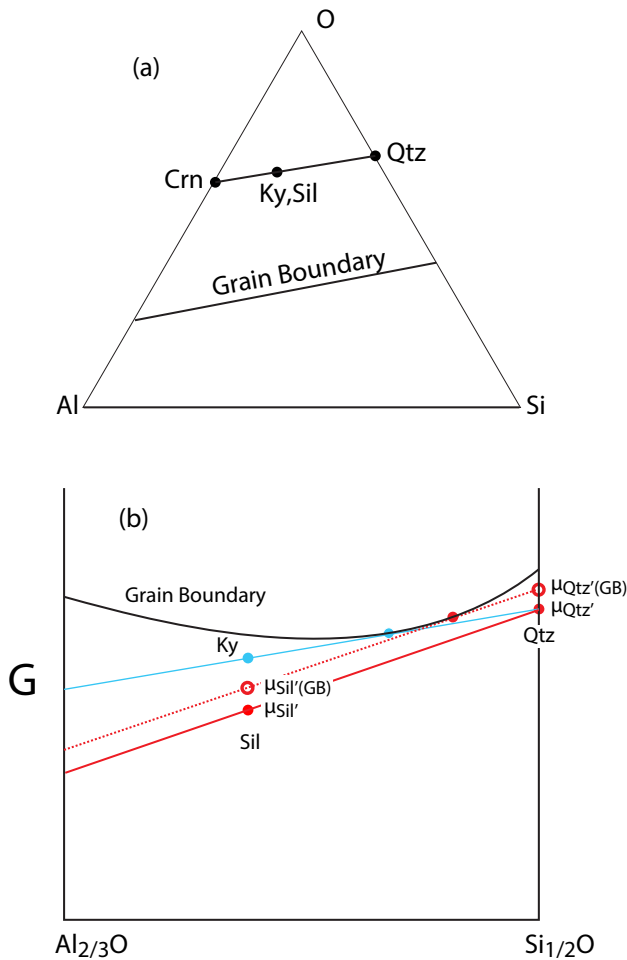


Fig. 3 **a** Composition triangle for the system Si–Al–O showing the plotting positions of quartz (Qtz), kyanite (Ky), sillimanite (Sil), corundum (Crn), and the grain boundary (GB). Note that the grain boundary is assumed to contain less oxygen than the solid phases. **b** G–X(Si_{1/2}O – Al_{2/3}O) diagram showing quartz, kyanite, and sillimanite and the projected grain boundary G–X curve. The blue tangent to quartz–kyanite–GB shows the initial condition before sillimanite nucleates. After sillimanite nucleates, the local sillimanite + quartz + grain boundary system will react until the grain boundary tangent (dotted red line) is parallel to the quartz + sillimanite tangent (solid red line). Note that the grain boundary composition at the local kyanite + quartz interface is more Al rich than the grain boundary composition at the local sillimanite + quartz interface. μ_{Qtz} , μ_{Sil} , $\mu_{Qtz'(GB)}$, and $\mu_{Sil'(GB)}$ are the chemical potentials of quartz and sillimanite in the solid phases and grain boundary, respectively

tangent to the grain boundary G–X curve is parallel to the tangent to the quartz–sillimanite tangent. This is so-called “parallel tangent” condition and represents the local equilibrium condition between the reacting solid phases and the grain boundary.

The above discussion assumes that the grain boundary components are oxides. According to Gibbs (1928), phase

components must be independently variable. Inasmuch as cations in the grain boundary are likely to be coordinated with oxygen in a variety of species in order to maintain electroneutrality, a permissible set of grain boundary components are the simple oxides, as used above. These components will be used throughout in the discussion of grain boundary chemistry. As mentioned above, the fact that the amount of oxygen in the grain boundary is constant, the use of oxide components yields identical results to those using individual cations and oxygen as grain boundary components.

The derivation of the parallel tangent as the condition of local equilibrium is as follows. A condition of heterogeneous equilibrium requires that at constant temperature and pressure, the change in free energy of the system must be 0 for any possible chemical change in the system. Using the association quartz + sillimanite + grain boundary in the system Si–Al–O as an example, this condition requires that

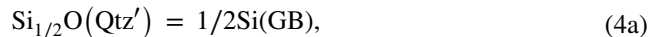
$$dG = 0 = \mu_{Qtz}dn_{Qtz} + \mu_{Sil}dn_{Sil} + \mu_{Si(GB)}dn_{Si(GB)} + \mu_{Al(GB)}dn_{Al(GB)}, \tag{2a}$$

where Si(GB) is SiO₂(GB) and Al(GB) is AlO_{3/2}(GB).

The two independent reactions that may occur between quartz, sillimanite and the grain boundary are



Or, written using one-oxygen formulas for the solid phases,



where the prime refers to the formula with only 1 oxygen. Because the condition of equilibrium is independent of how components are chosen, Eq. (2) can also be written as

$$dG = 0 = \mu_{Qtz'}dn_{Qtz'} + \mu_{Sil'}dn_{Sil'} + \mu_{Si(GB)}dn_{Si(GB)} + \mu_{Al(GB)}dn_{Al(GB)}. \tag{2b}$$

The stoichiometry of these reactions (4) requires that

$$-dn_{Qtz'} = 2dn_{Si(GB)} = d\xi_1, \tag{5a}$$

$$-dn_{Sil'} = 5dn_{Si(GB)} = \frac{5}{2}dn_{Al(GB)} = d\xi_2, \tag{5b}$$

where ξ_1 and ξ_2 are the progress variables for the two reactions. Substituting into Eq. 2b we have

$$dG = 0 = -\mu_{Qtz}d\xi_1 - \mu_{Sil}d\xi_2 + \mu_{Si(GB)} \left(\frac{1}{2}d\xi_1 + \frac{1}{5}d\xi_2 \right) + \mu_{Al(GB)} \frac{2}{5}d\xi_2. \tag{6}$$

Now, to achieve oxygen balance among the solid phases, the extent of reaction for both reactions must be equal and opposite. That is,

$$d\xi_1 = -d\xi_2, \tag{7}$$

so

$$dG = 0 = -\mu_{Qtz}d\xi_1 + \mu_{Sil}d\xi_1 + \mu_{Si(GB)} \left(\frac{1}{2}d\xi_1 - \frac{1}{5}d\xi_1 \right) - \mu_{Al(GB)} \frac{2}{5}d\xi_1. \tag{8}$$

Or

$$dG = 0 = \left[-\mu_{Qtz} + \mu_{Sil} + \frac{3}{10}\mu_{Si(GB)} - \frac{2}{5}\mu_{Al(GB)} \right] d\xi_1. \tag{9}$$

To compare the grain boundary tangent with that of the solid phases, it is necessary to define the chemical potentials of the solid phases in terms of the grain boundary components. That is,

$$\mu_{Qtz(GB)} = \frac{1}{2}\mu_{Si(GB)}, \tag{10a}$$

$$\mu_{Sil(GB)} = \frac{2}{5}\mu_{Al(GB)} + \frac{1}{5}\mu_{Si(GB)}. \tag{10b}$$

Substituting for $\mu_{Si,GB}$ and $\mu_{Al,GB}$ and rearranging we have

$$dG = 0 = [(\mu_{Qtz(GB)} - \mu_{Qtz}) - (\mu_{Sil(GB)} - \mu_{Sil})] d\xi_1. \tag{11}$$

Each quantity within the interior brackets is the difference in chemical potential between the solid phase and the grain boundary calculated for the same composition as the solid phase and these quantities are here defined as the affinities for the solid phases. That is,

$$Aff_{Qtz} = (\mu_{Qtz(GB)} - \mu_{Qtz}), \tag{12a}$$

$$Aff_{Sil} = (\mu_{Sil(GB)} - \mu_{Sil}). \tag{12b}$$

For the change in free energy to be zero for any extent of reaction ($d\xi_1$), the affinities have to be equal which is equivalent to the tangent to the solid phases being parallel to that of the grain boundary phase.

This result may seem at odds with the intuition that at equilibrium, the solid and grain boundary phases should lie on a common tangent. However, that condition is only valid if the two progress variables can operate independently. The constraint of constant oxygen requires that the progress on the two solid reactions is coupled. Therefore, even though the value of $\mu_{Qtz(GB)}$ is higher than that of μ_{Qtz} as shown in Fig. 3b, it is

not possible to precipitate quartz without also consuming sillimanite, which would increase the overall free energy of the system as indicated in the above equations.

It should also be noted that a similar result would be obtained were the constraint of constant volume rather than constant oxygen imposed on the system. In the case of constant volume, the two progress variables are constrained as

$$d\xi_1 = -V_R d\xi_2, \tag{13}$$

where

$$V_R = \frac{V_{Qtz}}{V_{Sil}}. \tag{14}$$

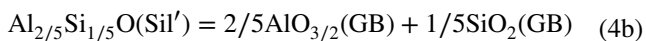
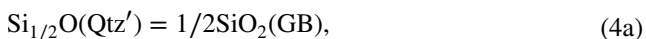
So that

$$dG = 0 = [(\mu_{Qtz(GB)} - \mu_{Qtz}) - (\mu_{Sil(GB)} - \mu_{Sil})V_R] d\xi_1 \tag{15}$$

As an example of these calculations, consider a “rock” in the system $SiO_2 - Al_2O_3$ that contains kyanite + quartz in equilibrium but at P–T conditions above the kyanite = sillimanite boundary (in this example the P–T conditions were chosen to be 650 °C, 0.5 GPa). In other words, the sillimanite isograd has been overstepped because sillimanite has not yet nucleated. The grain boundary composition is comprised of some amounts of both Si and Al but, in general, the actual composition is unknown. Initially, the grain boundary is assumed to be in equilibrium with the phases kyanite + quartz. Although the energetics of cations in a grain boundary are not known, values can be inferred for each specific example through application of the equilibrium assumption, which is valid because the absolute values of the thermodynamic properties of the grain boundaries is not critical to inferring the direction that the reactions will proceed, but rather only the values relative to the solid phases in the assemblage. That is, the initial equilibrium assemblage of kyanite + quartz + grain boundary is used to essentially calibrate the energetics of the grain boundary for this example. The procedure for this is described in detail in the Appendix II but basically involves assuming an arbitrary composition of the grain boundary (in this example, the grain boundary was assumed to have the composition $X_{SiO_2(GB)} = 0.6$, $X_{AlO_3/2(GB)} = 0.4$) and then calculating the chemical potentials for the grain boundary components that are consistent with this composition and the equilibrium with kyanite + quartz. It is important to note that the absolute values of the grain boundary thermodynamic parameters are not critical because the overall reaction progress is governed by the local reactions constrained by the conservation of oxygen. These calculations were done using program Gibbs3 (Spear and Wolfe 2022, Supplemental material) and the corresponding G–X diagram is consistent with the blue tangent line in Fig. 3b.

The modeling then assumes that sillimanite nucleates (Fig. 2). Sillimanite has a lower free energy than kyanite (as shown in Fig. 3b) and the calculated difference in G between sillimanite and kyanite at these conditions is 1010 J (=202 J/mol-O; SPaC thermodynamic data set of Spear and Pyle 2010) so sillimanite is expected to grow at the expense of kyanite with the grain boundary medium transporting the required elements between the two phases. In as much as the initial grain boundary composition is out of equilibrium with sillimanite, the goal is to determine how much sillimanite must grow in order to change the grain boundary composition such that the tangent to the grain boundary is parallel to the tangent to the quartz–sillimanite tangent. This calculation is done for each node and point in the entire grid (Fig. 2).

The relevant reaction(s) are those between adjacent phases at each node or grid point. The assemblage in Fig. 2 is relatively simple and the only possible reactions are between Al_2SiO_5 (sillimanite or kyanite) and quartz. Note that nodes where only quartz grains are adjacent will not react because, by definition, the affinities of each quartz grain relative to the grain boundary phase will be identical. For the local reaction between sillimanite (or kyanite) and quartz, the two independent reactions (written with one oxygen in each solid phase) are those given above:



The objective is to determine the extent of reaction (i.e., the change in the number of moles of the solid phases) that will result in the tangent to the grain boundary phase being tangent to the sillimanite + quartz tangent (red line in Fig. 3b). Oxygen balance is ensured by imposing the additional constraint: $\Delta\text{moles sillimanite} = -\Delta\text{moles quartz}$. The total number of moles of phases consumed or produced is dictated by the size of the effective bulk composition. In these models, it is assumed that the reactive volume for each phase is 1 nm wide. That is, the grain boundary is assumed to be 1 nm wide and the reactive part of sillimanite and quartz is assumed to be 1 nm into the crystals. The assumption that the reaction volume is 1 nm wide is entirely arbitrary and simply serves to scale the amount of phases consumed or produced as a function of reaction progress. That is, this assumption in no way impacts the overall reaction progress at various grid locations.

The tangent between sillimanite and quartz is straightforward to calculate because each phase is fixed composition. First, the chemical potentials of the grain boundary components are calculated assuming the activity is equal to the number of moles of the component:

$$\mu_{\text{SiO}_2(\text{GB})} = \mu^\circ_{\text{SiO}_2(\text{GB})} + RT\ln a_{\text{SiO}_2(\text{GB})}, \quad (16a)$$

$$\mu_{\text{AlO}_{3/2}(\text{GB})} = \mu^\circ_{\text{AlO}_{3/2}(\text{GB})} + RT\ln a_{\text{AlO}_{3/2}(\text{GB})}. \quad (16b)$$

Comparison with the chemical potentials of the solid phases requires the free energy of a fictive grain boundary compound with the same composition as the solid phase be computed, as described by Eqs. (10) above. Parallel tangency occurs when

$$\mu_{\text{Qtz}'(\text{GB})} - \mu_{\text{Qtz}'} = \mu_{\text{Sil}'(\text{GB})} - \mu_{\text{Sil}'}$$

The model proceeds by adopting an initial value for $\Delta\text{moles}(\text{sillimanite}) = -\Delta\text{moles}(\text{quartz})$ and calculating the change in grain boundary composition based on Eqs. (1) and the chemical potentials from Eqs. (16) and the affinities from Eqs. (10) and (12). The condition of parallelism (Eq. 11) is checked and the model iterates using Newton's method with the partial derivatives calculated explicitly until they are satisfied to within a tolerance of 1 J. The changes in the molar amounts of phases are recorded and visualized on the grid pallet (see Appendix I).

If three distinct phases exist at a node the calculation is somewhat more complicated, but essentially follows the outline presented above. Specifically, there are two independent reaction progress variables ($d\xi_1, d\xi_2$) and oxygen balance is achieved by requiring

$$0 = d\xi_1 + d\xi_2 + d\xi_3. \quad (17)$$

If one or more phases has variable composition (e.g., muscovite, garnet, biotite, etc.) then an additional set of calculations is required to ensure parallel tangency and will be discussed below.

Grain boundary diffusion modeling

Initially, there are no gradients in the composition of the grain boundary because the initial grain boundary is calculated to be in equilibrium with the existing (sillimanite-absent) assemblage. A new phase that nucleates will be out of equilibrium with the local grain boundary, which will initiate local reactions that will change the composition of the local grain boundary as described above. The compositional changes in the local grain boundary set up gradients that drive diffusion. As the diffusive flux reaches other phases (previously in equilibrium) these phases will no longer be in equilibrium with the local grain boundary and reactions will ensue that change the grain boundary composition at these locations.

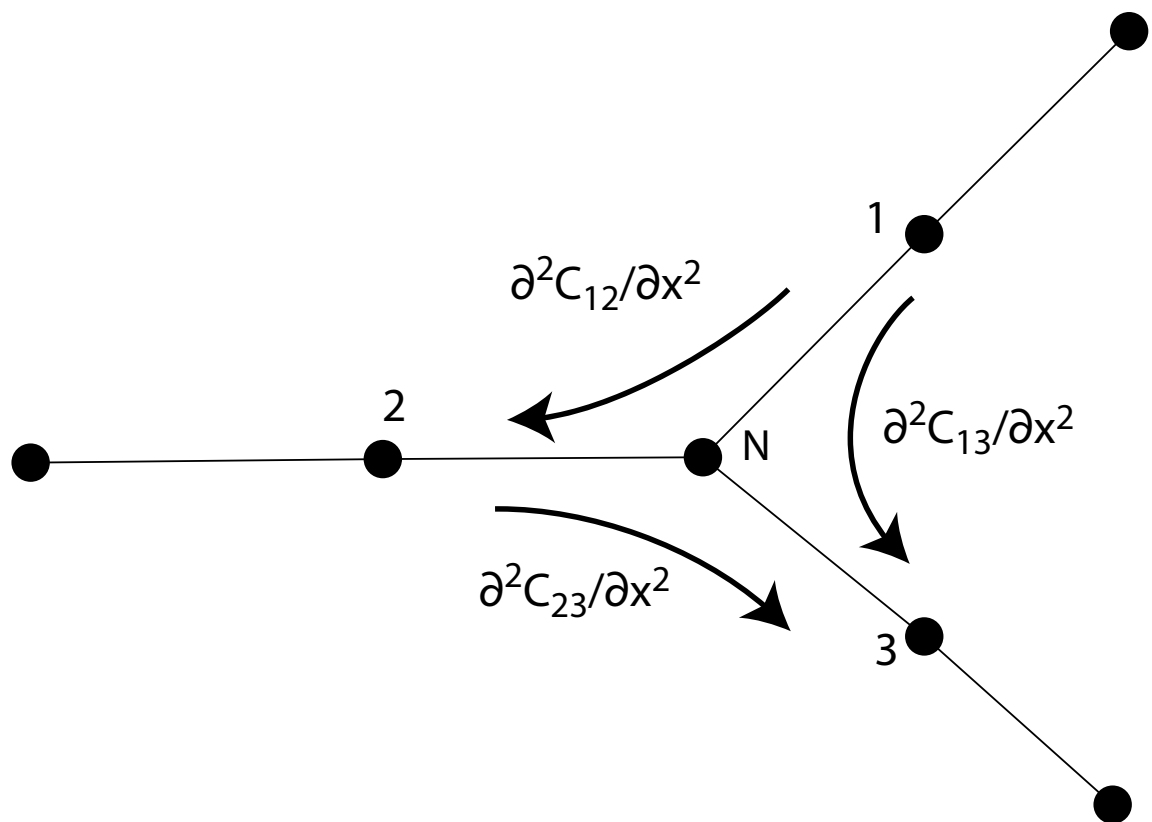


Fig. 4 Illustration of the finite difference diffusion calculation at a node (N). Black dots are grid points

The calculation of diffusive flux is accomplished by a simple, one-dimensional explicit approach using the finite difference approximations after Crank (1975). Diffusion along segments is calculated as.

$$C_i(t+1) = C_i(t) + D \left(\frac{\partial^2 C_i}{\partial X^2} \right) \Delta t,$$

Where C_i is the concentration of component “i” in the grain boundary and “t” is time. Where three segments intersect at a node, the change in composition at the node is calculated as the sum of the contributions from the three intersection segments (Fig. 4):

$$C_{i,N}(t+1) = C_{i,N}(t) + D \left(\frac{\partial^2 C_{i,12}}{\partial X^2} + \frac{\partial^2 C_{i,13}}{\partial X^2} + \frac{\partial^2 C_{i,23}}{\partial X^2} \right) \Delta t,$$

where $C_{i,N}$ is the concentration of component i at the node and $\partial^2 C_{i,12}/\partial X^2$ is the curvature of the concentration profile between grid points 1 and 2.

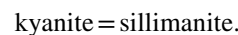
Diffusivities of atoms in grain boundaries are not known quantitatively but based on considerations of charge and ionic radius, it is assumed that the order of increasing diffusivity is

$$D_H > D_K \sim D_{Na} > D_{Fe} \sim D_{Mg} \sim D_{Mn} > D_{Ca} > D_{Al} > D_{Si}.$$

The absolute values of the diffusivities are not relevant to the modeling as the overall duration of diffusion between reaction steps in the modeling is user controlled. The relative values of the diffusivities are specified as model input parameters and can be adjusted to explore the parameter space.

Application to Carmichael (1969): the KASH system

Carmichael (1969) presented a reaction model for the reaction



by which kyanite was replaced by muscovite and sillimanite grew in and around muscovite elsewhere in the rock. His model called upon the relative immobility of Al compared with K whereby the local reactions conserved Al and K was transported through the grain boundary between the reaction sites. Carmichael’s interpretation emphasizes that the textural ramifications of even a simple reaction such as kyanite = sillimanite are dependent on local reactions and transport and cannot be quantified based on macroscopic

Fig. 5 Model for the reaction kyanite = sillimanite in the system KASH with only the phases quartz + muscovite + kyanite + sillimanite. **a** Initial grid configuration. **b** Grid configuration at the end of the model run. The configuration of the original grid is shown in (b) in red. Note the replacement of muscovite by sillimanite and the replacement of kyanite by muscovite. Numbered nodes (e.g., N2) are nodes referred to in the text. The green line (A–A') in (b) shows the path of the grain boundary composition profile depicted in Fig. 7

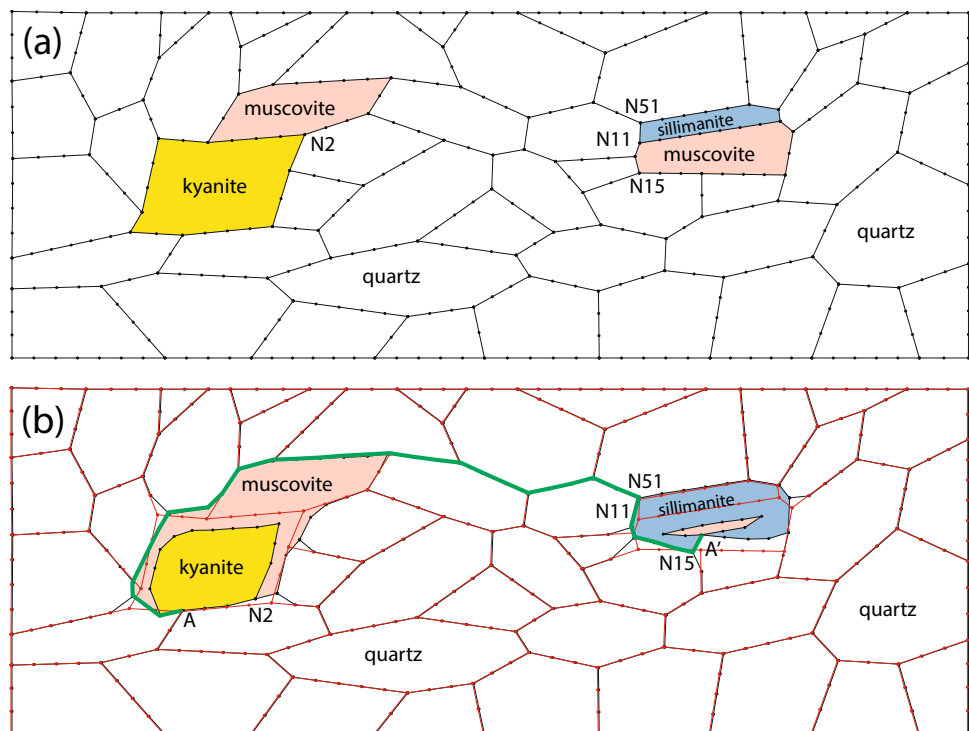


Table 1 Concentration of elements in the grain boundary at selected locations

Model step	Location	Assemblage	Si	Al	K	H
0 (initial)	Everywhere	n/a	0.5	0.1	0.2	0.2
1 (after reaction) ¹	N51	Sil + Qtz	0.50432	0.09423	0.20000	0.20000
1 (after reaction) ¹	N11	Sil + Ms + Qtz	0.49124	0.09240	0.21929	0.21929
1 (after reaction) ¹	N15	Ms + Qtz	0.5	0.1	0.2	0.2
1 (after diffusion)	N51	Sil + Qtz	0.50150	0.09719	0.20048	0.20083
1 (after diffusion)	N11	Sil + Ms + Qtz	0.50144	0.09691	0.20048	0.20017
1 (after diffusion)	N15	Ms + Qtz	0.50047	0.09839	0.20042	0.20073
1 (after diffusion)	N2	Ky + Ms + Qtz	0.50000	0.09999	0.20010	0.19991
450	N51	Sil + Qtz	0.49578	0.09455	0.21162	0.19805
450	N11	Sil + Ms + Qtz	0.49568	0.09463	0.21161	0.19807
450	N15	Ms + Qtz	0.49581	0.09422	0.21167	0.19831
450	N2	Ky + Ms + Qtz	0.49319	0.09869	0.21127	0.19685

1. Before diffusion

phase equilibria considerations. Carmichael's model is largely the inspiration for the modeling presented in this manuscript.

Carmichael (1969) balanced his open-system reactions on Al based on the assumption that Al is nearly "immobile" and locally conserved. He acknowledges that this results in volumetric changes which he believed could be accommodated by expulsion of $\text{Si}(\text{OH})_4$ from the system. Conservation of oxygen (or volume) in the reaction balancing alleviates this difficulty.

A simple model to explore the reaction kyanite = sillimanite in the presence of muscovite is shown in Fig. 5.

The initial model (Fig. 5a) has a single muscovite crystal adjacent to kyanite and, separated from kyanite, a crystal of muscovite adjacent to sillimanite. After iteration, the configuration is as shown in Fig. 5b. Muscovite has replaced kyanite, primarily around the edges and sillimanite has replaced muscovite, again primarily around the edges.

The initial configuration of the grid for the model (Fig. 5a) was constructed in the following sequence. The grid was constructed from a drawing of line segments as described in Appendix I with quartz, muscovite, kyanite, and sillimanite situated as shown with a grid spacing between grid points of 10 μm . The concentration of elements in the

Table 2 Diffusivities of grain boundary elements

Element	D_0 (m ² /sec)	E (kJ)
Si	1.0×10^{-6}	100
Al	2.0×10^{-6}	100
K	1.0×10^{-5}	100
H	1.0×10^{-4}	100
Fe	5.0×10^{-6}	100
Mg	5.0×10^{-6}	100
Mn	5.0×10^{-6}	100
Ca	5.0×10^{-6}	100
Na	1.0×10^{-5}	100

grain boundary were chosen arbitrarily and are listed in Table 1. It should be noted that the concentration of elements in the grain boundary is not known and the concentrations very likely vary along the grain boundaries according to the degree of lattice mismatch between adjacent crystals, but this in no way affects the outcome of the modeling because the major impactors are the results of the local reactions and the relative diffusivities of the elements in the grain boundaries.

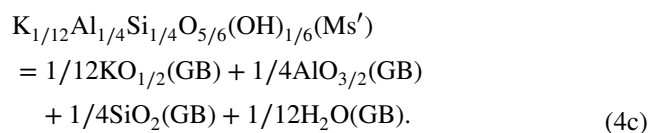
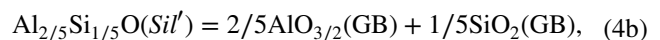
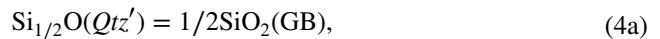
It is assumed in the modeling that the initial grain boundary composition is in equilibrium with the assemblage quartz + muscovite + kyanite. To implement this assumption, it is necessary to calculate the chemical potentials associated with the grain boundary components such that ΔG for the linearly independent reactions are all zero. This is done using Program Gibbs3 (Spear and Wolfe 2022; See Appendix II). The actual values of these chemical potentials are not critical to the model but this calculation is necessary to ensure that the initial grain boundary is in equilibrium with the assemblage with no sillimanite. At the P–T conditions of the model (650 °C, 0.5GPa), the free energy of sillimanite is approximately 1010 J/mol (202 J/mol-O) more negative than that of kyanite.

The diffusivities of the four elements in the grain boundary were arbitrarily chosen as shown in Table 2. These values are not well-constrained but are consistent with the experimental determination of Mg diffusion along quartz grain boundaries by Thomas and Watson (2014) and of carbon through periclase and olivine by Hayden and Watson (2008), although Carlson (2002) has inferred a considerably slower grain boundary diffusivity for Al. Again, the absolute values of the diffusivities do not impact model results, only the relative values. It is important to note that the diffusivity of K is assumed to be larger than that of Si or Al and the diffusivity of H is assumed to be an order of magnitude faster than that of K. Assuming rapid diffusivity of H essentially ensures that H will supply the charge balance required for the diffusion of the other elements.

The possible reactions in this grid involve two or three phases and the local reactions that occur at these associations are:

sillimanite or kyanite–quartz (e.g., node 51),
 muscovite–quartz (e.g., node 15),
 sillimanite or kyanite–muscovite (e.g., along segments where muscovite abuts sillimanite or kyanite),
 sillimanite or kyanite–muscovite–quartz (e.g., node 2 or node 11).

The reactions that occur at these locations are combinations of these reactions:



Locations where two phases occur are treated as above with $\Delta\text{moles}(\text{phase 1}) = -\Delta\text{moles}(\text{phase 2})$. Reactions in which three phases occur have two independent values of Δmoles that must be determined with the third molar amount constrained by $\Delta\text{moles}(\text{phase 3}) = -[\Delta\text{moles}(\text{phase 1}) + \Delta\text{moles}(\text{phase 2})]$ to ensure oxygen balance. Newton's method is used to find the solution with the partial derivatives calculated using an explicit approximation.

The model is run as a sequence of steps where each step is comprised of a reaction step and a diffusion step. The reaction step is calculated at every node and grid point where two or three distinct phases are adjacent. Reactions do not occur where adjacent phases are identical (e.g., along a quartz – quartz grain boundary) because there is no driving force for reaction among identical phases. The first reaction step will, of course, only produce changes in the grain boundary composition adjacent to sillimanite because the remainder of the grid is calculated to be in equilibrium with kyanite. For example, Table 1 gives the composition of the grain boundary after the initial reaction step at Nodes 51, 11, and 15. Node 15 (muscovite + quartz) shows no change because sillimanite is not present at that node. Node 51 (sillimanite + quartz) shows a small increase in Si, a small decrease in Al and no change in K or H. Node 11 (sillimanite + muscovite + quartz) shows a decrease in Si and Al and increase in K and H. It is significant to note that the direction of changes depends on the local assemblage (e.g., Node 11 vs Node 51) and also that these are not large changes in composition, but sufficient to drive the overall transformation in the model assemblages.

After the reaction step, the diffusion step results in modification of the grain boundary composition. The magnitude

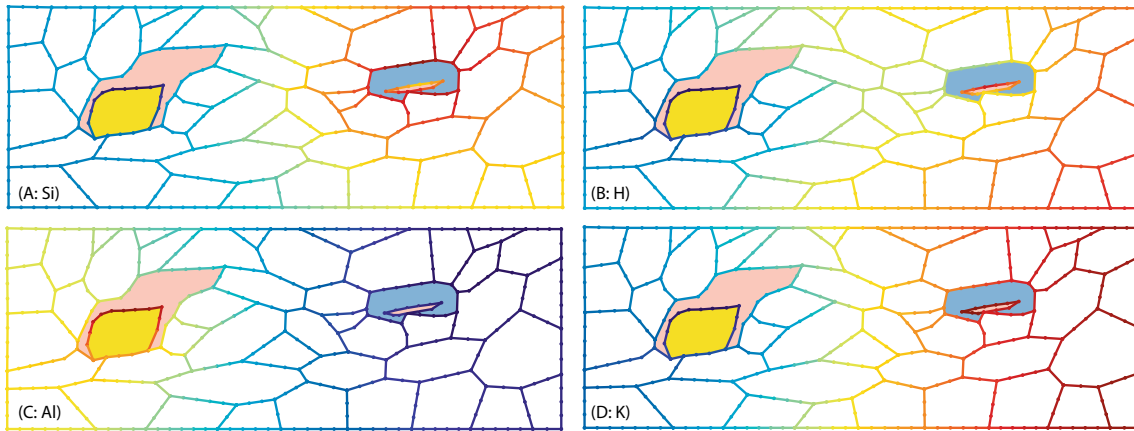


Fig. 6 Images of the grid at the model end (step 450) with grain boundaries colorized to show the distribution of elements. **a** Si; **b** H; **c** Al; **d** K. The color scale is adjusted to the minimum and maximum

range for each element (see Fig. 7) with the color spectrum from low-to-high being blue–green–yellow–orange–red

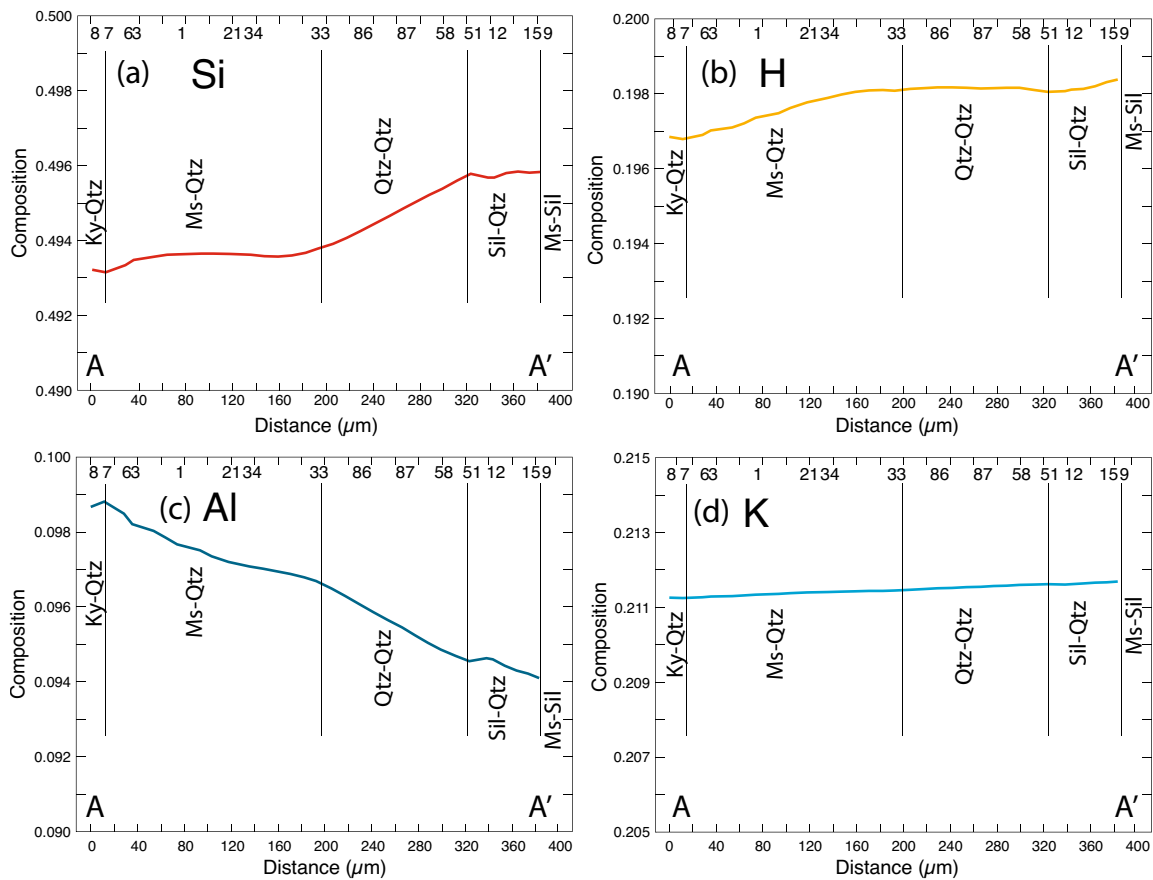


Fig. 7 Plots of Si, Al, H, and K concentrations along the grain boundary A–A' (green line in Fig. 5b). Distance is in μm. The low-to-high values for each element were used to scale the color spectrum in each

panel in Fig. 6. Note that the concentration gradient for each element is rather small and yet sufficient to drive the overall reaction

of a diffusion step (Δt) is calculated from the values of the largest diffusivity (D_H) to ensure numerical stability (following Crank 1975: $\Delta t D_H / \Delta x^2 < 0.5$ or $\Delta t < 0.5 \Delta x^2 / D_H$, where Δx is the spacing between grid points). In the model shown, there were 5000 diffusion steps run between each reaction step, which is approximately 16 years based on the diffusivities in Table 2. Note that the absolute value of this time frame is entirely arbitrary because the absolute values of diffusivities (Table 2) are arbitrary. This time frame for diffusion is user-specified and the implications of using a shorter diffusion time frame are discussed below. The concentrations of elements in the grain boundary at selected nodes after the first diffusion step are given in Table 1. As can be seen from the table, the diffusion step works toward homogenization of the grain boundary composition. After the initial diffusion step, the grain boundary composition at Node 2 (kyanite + muscovite + quartz) has changed slightly, which will promote the breakdown of kyanite and the growth of muscovite.

At the termination of the model (step 450), the composition of the grain boundary is not uniform but the direction of changes from the initial composition is similar at all points. The distribution of each element along the grain boundary is shown with a color spectrum in Fig. 6 with blue indicating low values and red indicating high values. As predicted, the highest values of Si and K are where sillimanite and muscovite coexist and the highest value of Al is along the kyanite–muscovite interface. Hydrogen (H) varies antithetically to Al and Si and maintains electroneutrality in the grain boundary. Quantitative values of the grain boundary composition are shown in Fig. 7 along the traverse A–A'

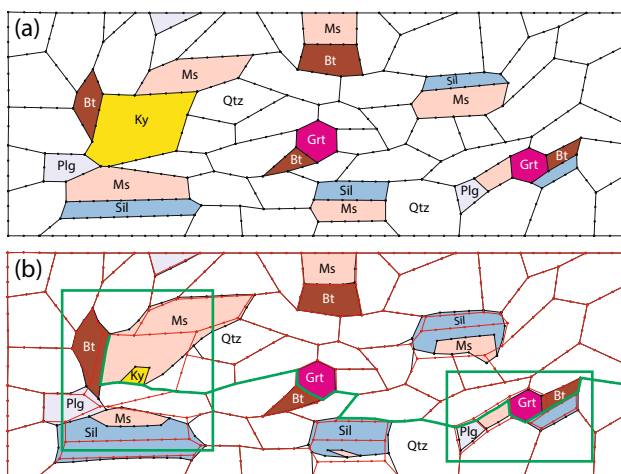


Fig. 8 Model grid in the system MnNCKFMASH with the phases quartz, muscovite, biotite, plagioclase, garnet, kyanite, and sillimanite. **a** Initial grid configuration. **b** Grid appearance at the end of the model run. The grid outlined in red shows the original grain boundary configuration from (a). Green boxes show areas of enlargement in Fig. 10. Green path shows grain boundary traverse in Fig. 11

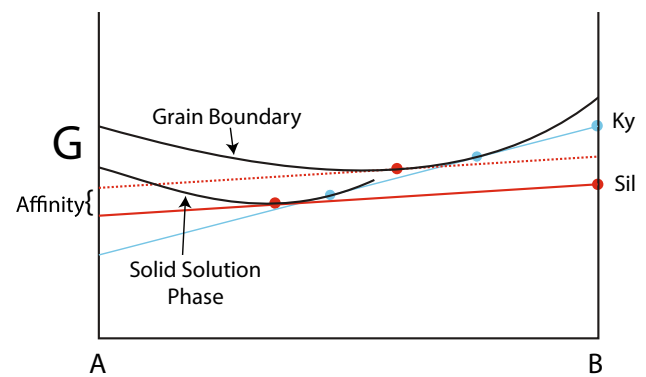


Fig. 9 Schematic G–X diagram showing how the composition of a solid solution phase that is constrained by the parallel tangent will change as equilibrium shifts from kyanite-bearing (blue line) to sillimanite-bearing (red lines)

(green line in Fig. 5b). All of the elements show relatively smooth gradients (also seen in Fig. 6) and all have changed from the initial values (Table 1). Specifically, Si, Al, and H have decreased and K has increased from the initial values of 0.5, 0.1, 0.2, and 0.2, respectively. Also note that the compositional gradients are not large revealing that only small gradients are required to drive the reaction of kyanite to sillimanite.

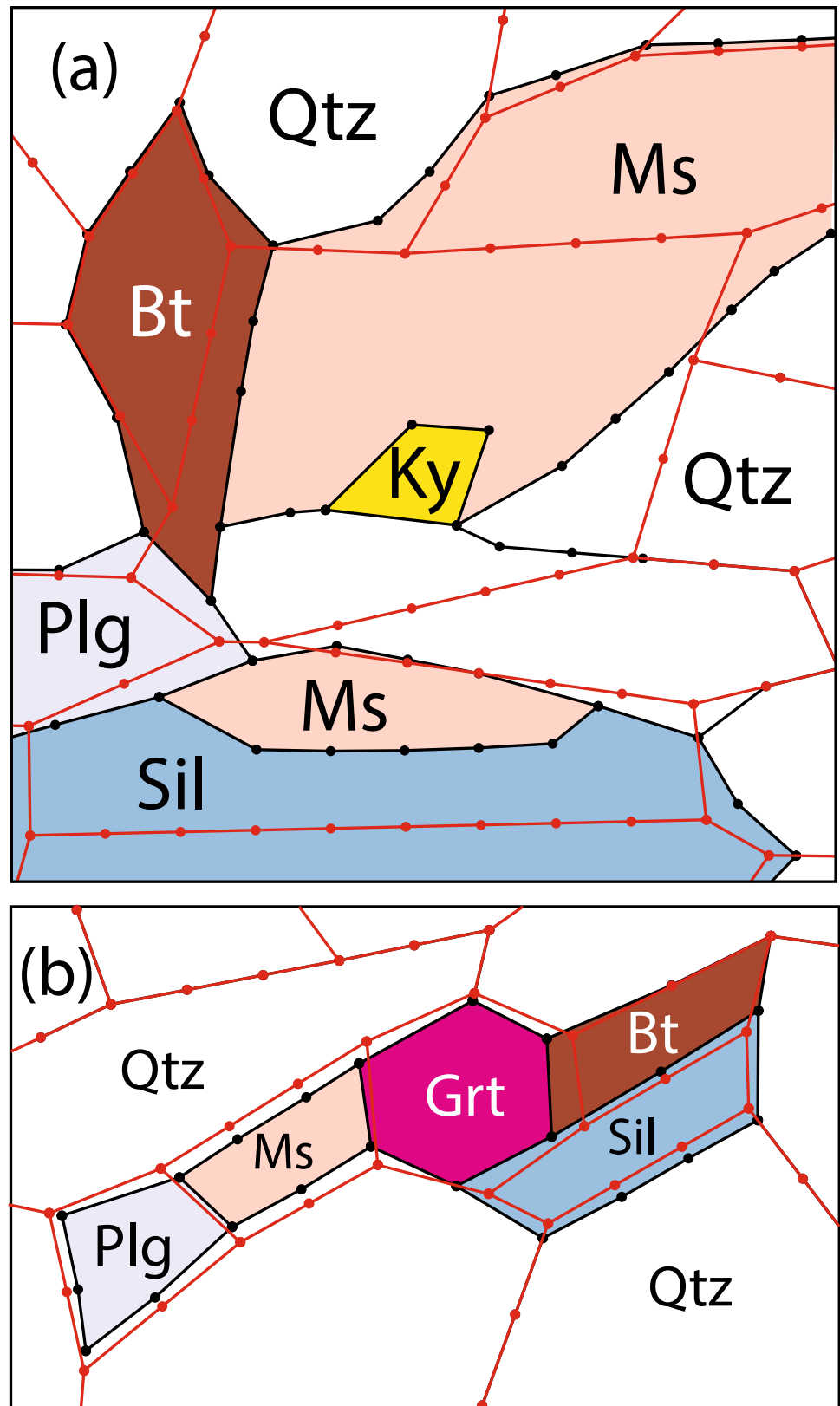
Models run with shorter diffusion time frames between reaction steps yield qualitatively similar results. Sillimanite replaces muscovite and muscovite replaces kyanite where they are adjacent. However, the extent of muscovite replacement of kyanite is less than that with longer diffusion times because the compositional gradients in the grain boundary are steeper.

Application to Carmichael (1969): the MnNCKFMASH system

Typical pelites contain additional system components and phases. To examine the impact of these additional phases, models have been run in the MnNCKFMASH system (Fig. 8). The grid was constructed as described above and phases assigned to polygons. The diffusivities used are shown in Table 2.

Calculations in the MnNCKFMASH system involve additional complexity because several of the phases display solid solution (i.e., muscovite, biotite, plagioclase, and garnet). In addition to the oxygen balance constraint as described above for reactions involving two or three phases, it is essential that the composition of the solid solution phases is appropriate to ensure that the tangent to the solid phases is parallel to the grain boundary tangent. That is, the composition of the solid phases adds

Fig. 10 Detail of two regions in the grid in Fig. 8. **a** Detail around kyanite remnant. **b** Detail around garnet crystal. In both diagrams the red lines and dots are the initial grid configuration



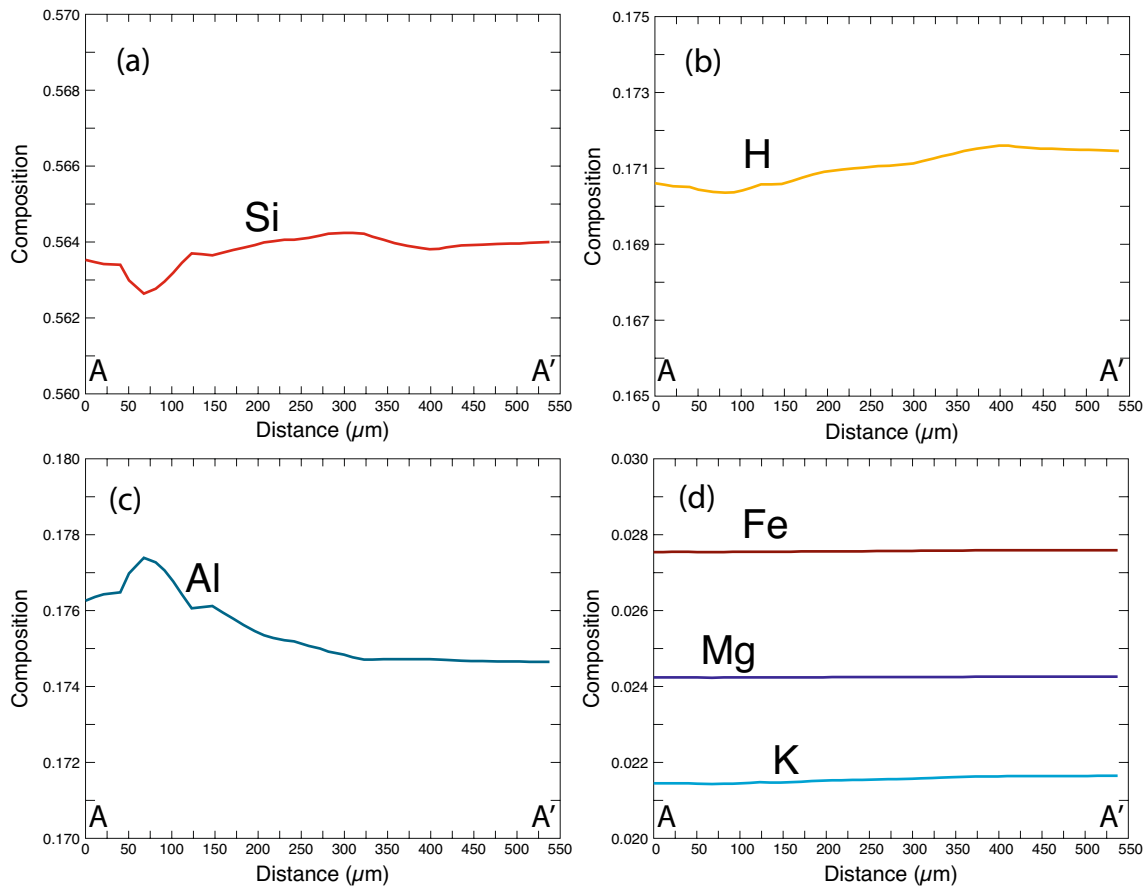


Fig. 11 Plots of Si, Al, H, K, Mg, and Fe concentrations along the grain boundary A–A' (green line in Fig. 8b). Concentrations of Na, Ca, and Mn are all low and nearly homogeneous (0.001–0.01)

Table 3 Initial and final composition of garnet and plagioclase

Garnet composition						
	Initial	Node 85	Node 83	Node 131	Node 133	Node 132
Prp	0.081	0.069	0.069	0.069	0.069	0.069
Alm	0.839	0.827	0.827	0.827	0.827	0.827
Sps	0.040	0.060	0.060	0.060	0.061	0.061
Grs	0.040	0.044	0.044	0.044	0.044	0.044
Plagioclase composition						
	Initial	Node 47	Node 6	Node 7	Node 23	Node 93
Ab	0.592	0.589	0.589	0.589	0.589	0.589
An	0.408	0.411	0.411	0.411	0.411	0.411

additional variables to the equations to be solved. This can be seen schematically in Fig. 9. The initial tangent in blue describes the equilibrium between kyanite, the grain boundary and the solid solution phase with the blue dot on the solution phase reflecting its composition. The parallel tangent in red represents the equilibrium with sillimanite with the red dot on the solution phase reflecting the

composition in equilibrium with sillimanite which, in this hypothetical example, is somewhat richer in component “A”.

Calculations involving solid solution phases are carried out iteratively by finding the composition of the phase that is parallel to the grain boundary tangent as shown in Fig. 9. This calculation also yields the affinity for the solution phase

as the difference between the tangent to the grain boundary and the solution phase (see Fig. 9). The values of Δmoles of the phases in the reaction are adjusted iteratively until all affinities are equal with the composition of the solution phase also on the parallel tangent.

The model results (Fig. 8b) reveal that kyanite is nearly completely consumed at the expense of sillimanite. Equally significant is the extent of reaction observed around the other phases in the rock. Figure 10 shows details of two regions in the model grid along with an overlay of the initial grid configuration. Figure 10a shows the region around the kyanite remnant. Comparison of the final crystal outlines with the initial configuration (red lines) reveals that not only does sillimanite replace muscovite in the transformation, but plagioclase, biotite, and quartz also grow at the expense of kyanite. Figure 10b shows a detail around a garnet crystal. At this location, sillimanite grows and muscovite is consumed. But plagioclase is also consumed, in contrast to plagioclase growth shown in Fig. 10a. Biotite grows against garnet but is consumed by sillimanite. Garnet is consumed by biotite and sillimanite but grows slightly against muscovite. Compositional gradients along the grain boundary depicted in Fig. 11 reveal only relatively minor variations in Si, Al, K, and H and virtually no variation in Fe or Mg. Concentrations of Mn, Na, and Ca (not shown) also show very little variation along the grain boundary.

Additionally, the compositions of solid solution phases change as a consequence of the reaction kyanite = sillimanite as shown in Table 3. Compared with the initial composition, which was in equilibrium with kyanite, the final composition of garnet is slightly enriched in Mn and depleted in Fe and Mg and plagioclase is slightly more An rich, although the change is not large. This compositional change is due to the change in the local composition of the grain boundary. It is also clear that the compositions do not vary with position in the grid because of the similarity of the grain boundary composition. Nevertheless, the small changes in garnet composition would be detectable using the electron microprobe and might (erroneously) be attributed to a process other than the transformation of kyanite to sillimanite.

These results carry profound implications for textural interpretations of metamorphic parageneses. Even though the whole-rock reaction is the simple transformation of kyanite to sillimanite, the other phases in the rock are seen to both grow and be consumed depending on their locations. Clearly, any interpretations of metamorphic parageneses based on mineral compositions must take this complex behavior into account.

Discussion

To reiterate, the essential aspects of the model are these:

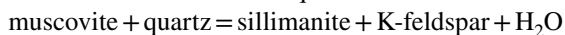
(1) All reactions are local and only occur among adjacent phases. (2) Reactions are balanced to conserve oxygen, which guarantees grain boundaries do not grow with reaction progress. The assumption of constant volume would provide similar results but is more cumbersome to model.

(3) The driving force for reactions is the differences in affinity among adjacent phases and the grain boundary. Affinities are calculated relative to the tangent to the grain boundary phase and reaction progress ceases (locally) when the affinities of all adjacent phases are equal. (4) Local reactions result in the growth or consumption of crystals and the change of grain boundary composition. (5) Grain boundary diffusion is driven by differences in grain boundary composition, which is controlled by the local reactions. Grain boundary diffusion initiated at one reaction local alters the composition of the grain boundaries elsewhere in the rock, which initiates reactions at these localities. (6) Reactions should proceed until all affinities are zero, at which point the rock will be in bulk thermodynamic equilibrium.

Other published studies have focused on grain boundary diffusion as the controlling process in the evolution of metamorphic assemblages and textures. As discussed above, Carmichael (1969) proposed that the relative immobility of Al compared with K could explain the common textural observation whereby kyanite is replaced by muscovite as sillimanite grows in contact with muscovite elsewhere in the rock. Although largely qualitative in approach, the implication of Carmichael's work is the importance of grain boundary diffusion in controlling the textural evolution of metamorphic recrystallization. More quantitative approaches have been detailed by Foster (1986, 1990, 1991, 1999) using a macroscopic approach involving chemical potential gradients with results very similar to those presented here (Foster 1990). Carlson (1989, 1991) has argued for the importance of grain boundary diffusion in the growth of metamorphic porphyroblasts and has used a grain boundary model to estimate the grain boundary diffusivity of Al from corona textures. However, the present study represents the first coupled local reaction modeling with quantitative grain boundary diffusion.

The models described above suggest some important implications for the interpretation of metamorphic textures. First, it is clear from the work of Carmichael (1969), Foster (1986, 1990, 1991), Carlson (1989, 1991) and this study that reaction pathways are complex. Even the simple polymorphic transition of kyanite to sillimanite generates local reactions not involving these phases but that result in the growth and/or consumption of phases in various locations in the rock (e.g., Figs. 8, 10).

The initiation of these complex reaction paths may be caused by the nucleation of a new phase that is out of equilibrium with the current assemblage. In this example the nucleating phase is sillimanite, but the same complexity will arise with the nucleation of any new phase. Nucleation requires a positive affinity to overcome the nucleation barrier and the buildup of affinity from overstepping the kyanite = sillimanite boundary is relatively meager, as pointed out by Pattison et al. (2011). For example, at the conditions of the modeling described here (650 °C, 0.5 GPa = 87 degrees of overstepping of the kyanite = sillimanite boundary) the affinity for sillimanite nucleation is only 202 J/mol-O. In contrast, the affinity for the nucleation of sillimanite from muscovite + quartz via the reaction



is considerably more rapid and with a similar ΔT of overstepping (87 degrees), the affinity is nearly 2 kJ/mol-O. This may explain why sillimanite is much more likely to nucleate on muscovite rather than kyanite. Of course, any other process that results in a change from existing equilibrium conditions such as rapid changes in P or T or metasomatic infiltration will also trigger similar complex reaction paths as the rock attempts to return to equilibrium.

Another important conclusion of the present modeling is that the interpretation of metamorphic textures is not always straight forward and requires careful scrutiny. This modeling, as well as those discussed by Foster (1986, 1990, 1991, 1999) reveal that a given phase may grow in one part of a rock at the same time it is being consumed elsewhere. Mineral resorption or overgrowths, therefore, may not be the result of external inputs (e.g., fluid metasomatism) or retrograde processes. Rather, complex and subtle textures may result from a simple polymorphic transition triggered by the nucleation of a new phase, changes in P or T or infiltration.

Supplementary Information The online version contains supplementary material available at <https://doi.org/10.1007/s00410-024-02100-9>.

Acknowledgements This work was funded in part by grant 2147526 from the National Science Foundation (to Spear) and funds from the Edward P. Hamilton Chair (at Rensselaer). Tom Foster, John Brady, and Jack Cheney provided insightful and critical comments on an early version of the manuscript that greatly helped improve the presentation and the manuscript was significantly improved thanks to a thorough and thoughtful review by Fred Gaidies.

Funding Division of Earth Sciences, 2147526, Frank S. Spear

Data availability Details of the grid construction and evolution are presented in Appendix I and a discussion of the calibration of the grain boundary chemical potentials is presented in Appendix II (Supplemental material).

Declarations

Conflict of interest None.

Open Access This article is licensed under a Creative Commons Attribution 4.0 International License, which permits use, sharing, adaptation, distribution and reproduction in any medium or format, as long as you give appropriate credit to the original author(s) and the source, provide a link to the Creative Commons licence, and indicate if changes were made. The images or other third party material in this article are included in the article's Creative Commons licence, unless indicated otherwise in a credit line to the material. If material is not included in the article's Creative Commons licence and your intended use is not permitted by statutory regulation or exceeds the permitted use, you will need to obtain permission directly from the copyright holder. To view a copy of this licence, visit <http://creativecommons.org/licenses/by/4.0/>.

References

- Carlson WD (1989) The significance of intergranular diffusion to the mechanisms and kinetics of porphyroblast crystallization. *Contrib Miner Petrol* 103:1–24
- Carlson WD (1991) Competitive diffusion-controlled growth of porphyroblasts. *Mineral Mag* 55:317–330
- Carlson WD (2002) Scales of disequilibrium and rates of equilibration during metamorphism. *Am Miner* 87:185–204
- Carlson WD, Hixon JD, Garber JM, Bodnar RJ (2015) Controls on metamorphic equilibration: the importance of intergranular solubilities mediated by fluid composition. *J Metamorph Geol* 33:123–146. <https://doi.org/10.1111/jmg.12113>
- Carmichael DM (1969) On the mechanism of prograde metamorphic reactions in quartz-bearing pelitic rocks. *Contrib Miner Petrol* 20:244–267
- Castro AE, Spear FS (2017) Reaction overstepping and reevaluation of the peak P-T conditions of the blueschist unit Sifnos, Greece: Implications for the Cyclades subduction zone. *Int Geol Rev* 59:548–562. <https://doi.org/10.1080/00206814.2016.1200499>
- Chu X, Akça O, Gaidies F, Gennaro I, Ji W (2023) Thermal pulse induced by emplacement of Ramba leucogranites in southern Tibet. *J Metamorph Geol* 41(1):121–141. <https://doi.org/10.1111/jmg.12690>
- Crank J (1975) *The Mathematics of Diffusion*. Oxford University Press, London, p 414
- Foster CT Jr (1986) Thermodynamic models of reactions involving garnet in sillimanite/staurolite schist. *Mineral Mag* 50:427–439
- Foster CT, Jr. (1990) Control of material transport and reaction mechanisms by metastable mineral assemblages: An example involving kyanite, sillimanite, muscovite and quartz. In: *Special Publication No 2, The Geochemical Society*, pp 121–132
- Foster CT Jr (1991) The role of biotite as a catalyst in reaction mechanisms that form sillimanite. *Can Mineral* 29:943–963
- Foster CT (1999) Forward modeling of metamorphic textures. *Can Mineral* 37:415–429
- Gaidies F, Pattison DRM, de Capitani C (2011) Toward a quantitative model of metamorphic nucleation and growth. *Contrib Miner Petrol* 162(5):975–993. <https://doi.org/10.1007/s00410-011-0635-2>
- Gibbs JW (1928) *The Scientific Papers of J. Willard Gibbs*. Volume One. Thermodynamics. Yale University Press, New Haven 434pp
- Hayden LA, Watson EB (2008) Grain boundary mobility of carbon in Earth's mantle. A possible carbon flux from the core. *Proceedings of the National Academy of Sciences* 105(25):8537–8541. <https://doi.org/10.1073/pnas.0710806105>
- Hollister LS (1969a) Metastable paragenetic sequence of andalusite, kyanite, and sillimanite, Kwoiek area, British Columbia. *Am J Sci* 267:352–370
- Hollister LS (1969b) Contact metamorphism in the Kwoiek area of British Columbia: An end member of the metamorphic process. *Geol Soc Am Bull* 80:2465–2494

- Pattison DRM, Spear FS (2018) Kinetic control of staurolite- Al_2SiO_5 mineral assemblages: Implications for Barrovian and Buchan metamorphism. *J Metamorph Geol* 36:667–690. <https://doi.org/10.1111/jmg.12302>
- Pattison DRM, de Capitani C, Gaidies F (2011) Petrological consequences of variations in metamorphic reaction affinity. *J Metamorph Geol* 29(9):953–977. <https://doi.org/10.1111/j.1525-1314.2011.00950.x>
- Pattison DRM (2023) Problems with Barrovian metamorphism. In: Palin RM (ed) *Metamorphic Studies Group Research in Progress*, vol., Oxford, UK, p 36
- Spear FS (1993) *Metamorphic Phase Equilibria and Pressure-Temperature-Time Paths*. Mineralogical Society of America, Washington, D. C., p 799
- Spear FS, Pattison DRM (2017) The implications of overstepping for metamorphic assemblage diagrams (MADs). *Chem Geol* 457:38–46. <https://doi.org/10.1016/j.chemgeo.2017.03.011>
- Spear FS, Pyle JM (2010) Theoretical modeling of monazite growth in a low-Ca metapelite. *Chem Geol* 266:218–230. <https://doi.org/10.1016/j.chemgeo.2010.02.016>
- Spear FS, Wolfe OM (2022) Nucleation theory applied to the development of contrasting garnet crystal densities. *Contrib Miner Petrol* 177:14. <https://doi.org/10.1007/s00410-021-01879-1>
- Spear FS, Thomas JB, Hallett BW (2014) Overstepping the garnet isograd: a comparison of QuiG barometry and thermodynamic modeling. *Contrib Miner Petrol* 168(3):1–15. <https://doi.org/10.1007/s00410-014-1059-6>
- Thomas JB, Watson EB (2014) Diffusion and partitioning of magnesium in quartz grain boundaries. *Contributions to Mineralogy and Petrology* 168:12 pp. <https://doi.org/10.1007/s00410-014-1068-5>
- Thompson CV, Spaepen F (1983) Homogeneous crystal nucleation in binary metallic melts. *Acta Metall* 31:2021–2027
- Waters DJ, Lovegrove DP (2002) Assessing the extent of disequilibrium and overstepping of prograde metamorphic reactions in metapelites from the Bushveld Complex aureole, South Africa. *J Metamorph Geol* 20(1):135–149. <https://doi.org/10.1046/J.0263-4929.2001.00350.X>
- Wolfe OM, Spear FS (2018) Determining the amount of overstepping required to nucleate garnet during Barrovian regional metamorphism, Connecticut Valley Synclinorium. *J Metamorph Geol* 36:79–94. <https://doi.org/10.1111/jmg.12284>

Publisher's Note Springer Nature remains neutral with regard to jurisdictional claims in published maps and institutional affiliations.